Cyclic behaviour of precast RC connections

Manoj K. Joshi, C.V.R. Murty and M. P. Jaisingh

Earthquake damages of precast structures can be attributed to poor connections between precast elements and also between precast elements and lateral load-resisting system. In this context, four experiments were performed on precast and corresponding monolithic exterior beam-column joint sub-assemblage specimens. The schemes for the anchorage of beam bars were different in the two sets of specimens. Further, in precast specimens, the connectivity of reinforcement bars between beam and column was achieved by welding the exposed bars of the components in the joint region. Under displacement-controlled pseudo-static loading, the precast specimen with beam bars anchored into the column performed better than the precast specimen with continuous U-bars as beam reinforcement; this performance of the former was comparable to that of the corresponding monolithic specimen.

Keywords: *Cyclic behaviour, precast structures, beam-column joint*

The lateral load resistance in precast frame buildings is critically dependent on the cast-in-situ jointing of the precast units designed for gravity loads. Although many precast buildings were undamaged during the 1994 Northridge earthquake and 1987 Whittier earthquake, most precast structures failed in 1995 Kobe and 1988 Armenia earthquakes due to poor connections between the precast elements themselves and between the precast elements and lateral load-resisting system[1].

Experimental research

Past studies on hysteretic behaviour of connections classify under two main categories, namely

(i) wet connections, in which fresh concreting or grouting is done at the site to cover the exposed reinforcements in the connection region

(ii) dry connections, in which only mechanical connections are used.

Dry connections detailed for carrying moments and shear forces, showed same displacement ductility but more energy dissipation characteristics compared to the monolithic connections[2]. The wet connections consisted of three types, namely

- *post-tensioned connections* (members are interconnected with post-tensioning cables), which showed more displacement ductility but less energy dissipation characteristics, *Fig* 1*(a)* compared to the monolithic connections[3]
- *threaded rebar connections* (members are interconnected with bolting over threaded rebars passing across

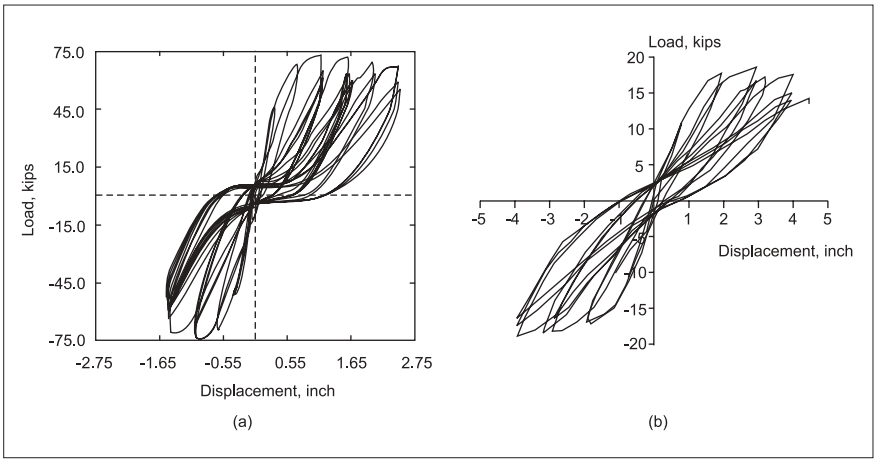

Fig 1 Hysteretic response of beam-column connection sub-assemblages under transverse loading: (a) Post-tensioned connection[3] (b) Connection using continuous threaded rebars and subsequent grouting[4]

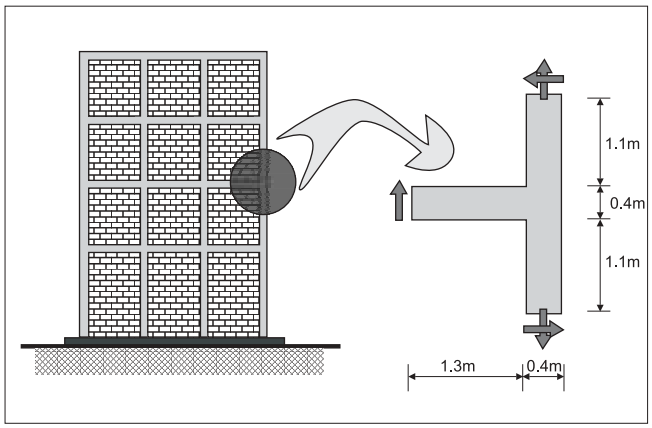

Fig 2 Exterior beam-column sub-assemblage of an RC frame building, geometry and forces acting on it when it swings from right to left

members), which showed more energy dissipation characteristics, *Fig* 1*(b)*[4]

- *cast in-situ connections* (beam and column segments are precast and then interconnected with cast in-situ jointing) which showed a wide range of performance. The connections of category cast-in-situ are in turn based either on welding of reinforcement or by using 90° hooks of adequate lengths for anchoring the reinforcement bars across the specimen.

Design provisions

The Indian codes of practice give guidelines for design and construction of precast reinforced or prestressed concrete ribbed, cored and waffle units[5,6]. Although seismic analysis and design requirements are given for precast structures involving large panel prefabricates, design and details of connections are not specified for precast structures in seismically-active areas[7,8]. On the other hand, among the international codes, NEHRP code permits both elastic and inelastic designs of connections[9]. For the design of precast members, the UBC and ACI code provisions recommend that all loading and restraint conditions be considered from initial fabrication to completion of structure, and provide strength requirements for various connections[10,11].

The New Zealand code of practice recommends that precast elements be designed based on all critical stages of loading[12]. Load-paths need to be provided in the structure for effective transfer of seismic forces through the lateral-load resisting system to maintain the structural integrity. The NZS code recommends two-fold general specification on fixings, namely

(i) resistance to all applied forces and accommodation of imposed deformations

(ii) accommodation of structural damage within a permitted level of strength degradation.

Connections are designed between the precast elements themselves and between the precast and cast in-situ elements for

- controlling the cracking
- developing a flexural failure mode through yielding of steel
- providing sufficient horizontal capacity in connectors to transfer the effects of horizontal seismic forces.

For column bases and horizontal joints, vertical steel is specified. Also, for vertical precast wall panels, component strength requirements and number of ties are specified. The code also recommends the general requirements of ductility capacity, energy dissipating mechanisms and capacity design principles to be applied in the design method.

Scope of present study

The present study aims at identifying a suitable technique for connecting precast beam and column components at an exterior joint in moment resisting frames in high seismic areas. The study investigated two connection techniques; two

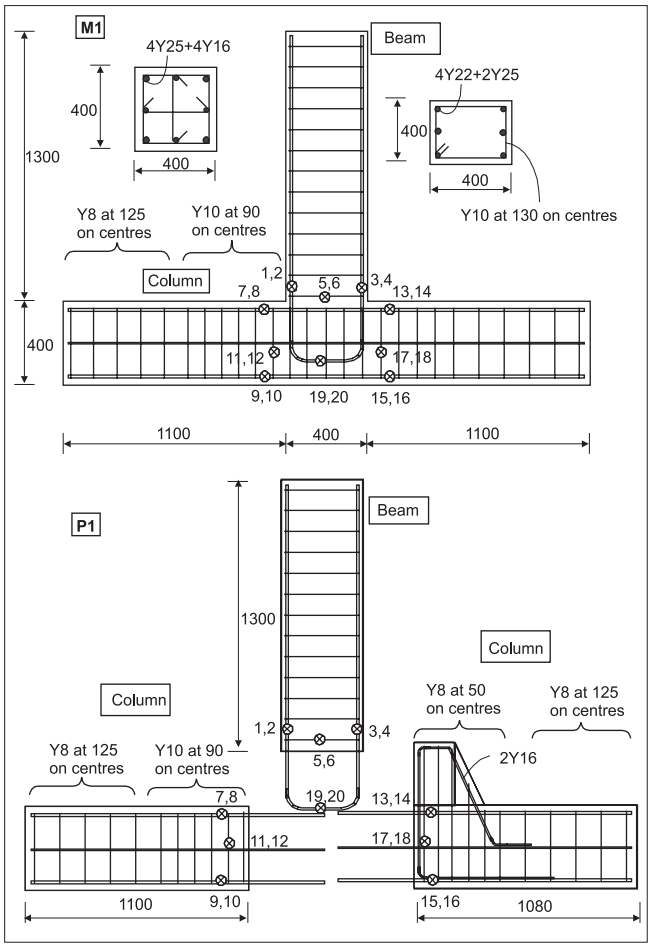

Fig 3 Details of geometry and reinforcement of the specimens M1 and P1. Clear cover to beam and column reinforcements are 25 mm and 40 mm, respectively, ⊗ denotes location of strain gauge

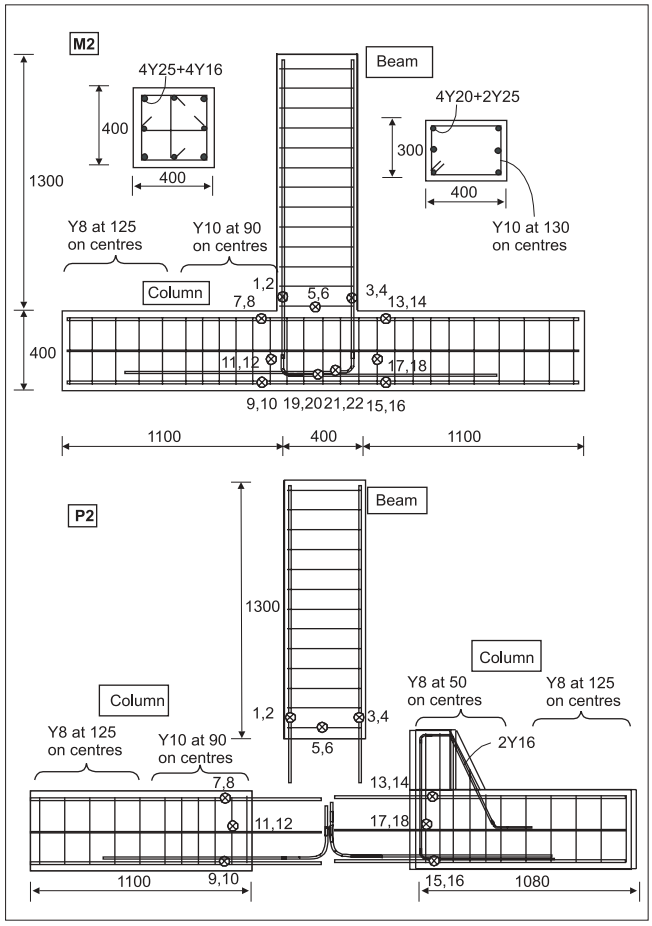

Fig 4 Details of geometry and reinforcement of the specimens M2 and P2. Clear cover to beam and column reinforcements are 25 mm and 40 mm, respectively. ⊗ denotes location of strain gauge

precast and corresponding monolithic specimens were prepared and subjected to pseudo-static loading to investigate the effectiveness of the same.

Present experimental study

Specimen properties

Material characteristics

OPC 43 grade cement from the same stock was used in all specimens. The grade of concrete used was M25 with a water-cement ratio of 0.5 for the design mix. The 28-day average compressive strengths of the cubes of two monolithic specimens M1 and M2 were 28.1 MPa and 31.3 MPa respectively, and those of the precast specimens P1 and P2 were 27.7 MPa and 32.4 MPa respectively. Reinforcement steel used in all the four specimens was of grade *Fe* 415; yield and ultimate strengths of 20 mm bars were 500 MPa and 630 MPa respectively, while those of 25 mm bars were 476 MPa and 641 MPa respectively.

Geometry and reinforcement detailing

The specimens had a strong-column weak-beam configuration, and represented the exterior beam-column joint of the four-storey reinforced concrete building, *Fig* 2. The column portion was 2.6 m long with a 400 mm × 400 mm cross-section and the beam portion was 1.3 m long with a 300 mm × 400 mm cross-section. Two types of detailing were used in the specimens. In the first type of detailing a single U-bar is used as both top and bottom beam reinforcement, as in the specimens M1, *Fig* 3*(a)*, and P1, *Fig* 3*(b)*; here, letters M and P stand for monolithic and precast respectively. The other type of detailing conforms to the Indian Standard code for ductile detailing of RC sections, as in the specimens M2, *Fig* 4*(a)*, and P2, *Fig* 4*(a)*[13]. Detailed descriptions of the specimens and their preparations are documented elsewhere[14].

Experimental setup

The specimens were loaded with the column stub horizontal and the beam stub vertical, *Fig* 5. The axial movement of the column was restrained at its ends by stiff supports fixed to the strong floor by steel studs. The ends of the column stub were supported by rollers equidistant from the beam centre. In specimen M1, plates were also provided along with the rollers to provide a larger bearing surface to the specimen.

In the testing of precast specimen P1, the spacer piece of the collar arrangement was eliminated as it became unstable in the second cycle of 20 mm displacement. Also, the plates between the column stub and the strong floor at the location of rollers were eliminated that facilitated an increase in lever arm. This was necessary because during the testing of the precast specimen P1 the actuator load capacity of 250 kN was reached in the positive direction beyond 20 mm displacement cycle. An increased lever arm was expected to induce higher displacement under the same transverse load on the beam and with the same load capacity of the actuator.

Loading sequence

The sub-assemblage specimens were subjected to cyclic displacement- controlled lateral loading applied at the end of the beam. A 250-kN capacity MTS hydraulic actuator with a displacement range of ± 150 mm was used. Two loading histories were adopted. The first one was used for the monolithic specimens. The loading history consisted of displacement cycles of $\pm$ 1, ±2, ±3, ±5, ±7.5, ±10, ±15, ±20,

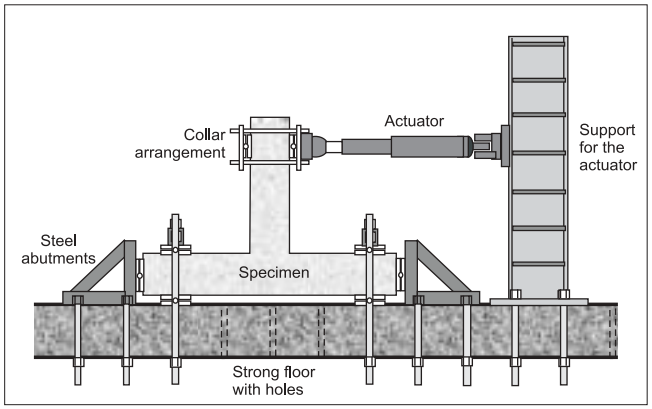

Fig 5 Experimental set-up used for cyclic loading of specimens

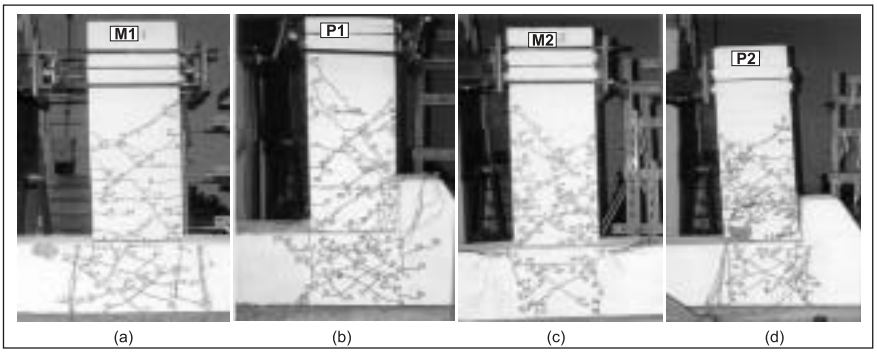

Fig 6 Crack pattern in the four specimens at the end of displacement loading

Responses measured

Displacements were measured in the specimen by LVDTs. LVDT 1 and LVDT 2 were used to measure the displacement at the point of application of load in the positive and negative displacement directions respectively. LVDT 6 was used to measure the displacement, if any, of the specimen support. The displacement at the actuator support was measured using LVDT7. LVDTs 3, 4 and 5 were used to measure the displacement at locations along the beam.

±25, ±30, ±40, ±50, ±60, ±70 and ±90 mm. Three cycles were applied at each of these displacement levels.

The presence of corbels in the precast specimens resulted in an unsymmetrical strength of the specimen in the positive direction of loading; thus, the displacement could not be increased beyond 20 mm in the positive direction as the actuator load capacity of 250 kN was reached. A revised loading history was applied for the displacement cycles beyond those of 20 mm. In the positive direction, displacement was increased till either the maximum load capacity or the desired displacement was reached first. In the negative direction, displacement was increased as in the case of monolithic specimens.

As the testing of the precast specimen P1 was conducted in two stages with the load applied at different levels in both the experiments, LVDT 8 and LVDT 9 were added to measure the response at the earlier load application level. LVDT1 and LVDT2 were used to measure the displacement at the new point of application of the load. Strain gauges were pasted on longitudinal and shear reinforcements for measuring strains in them at the probable plastic hinge sections.

Experimental observations

The various observations made during the cyclic loading of the specimens are described below. The diagrams of crack patterns observed in the various specimens at the end of the experiment are shown in *Fig* 6. For both specimens M1 and

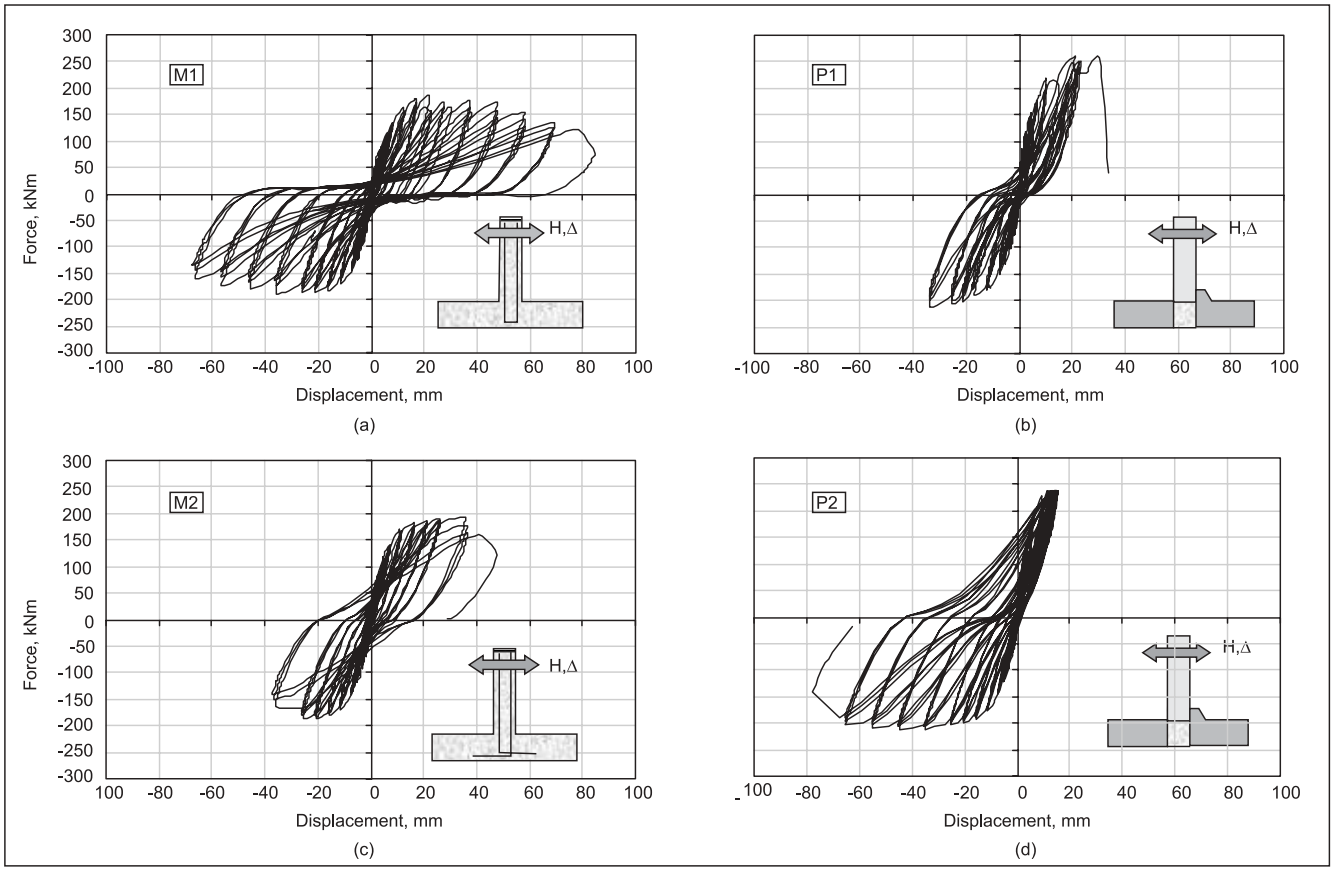

Fig 7 Hysteresis loops of the four specimens studied

P1, the first flexural cracks appeared in the 3 mm-displacement cycle at the junction of the beam and the column. The first crack runs across the full depth of the beam for the specimen M1. Flexural cracks in the beam away from the beam-column junction were also observed in the 5 mm, 7.5 mm and 10 mm displacement cycles for both the specimens. For the specimen P1, flexural cracks also appeared in the 25 mm and 30 mm displacement cycles. The first shear crack appeared in the 10 mm displacement cycle for both the specimens in both the beam and the joint regions.

For both specimens M2 and P2, the first crack develops in the 2 mm displacement cycle with the crack forming at the junction of beam and column for M2 and at the junction of the beam and the corbel for P2 respectively. Flexural cracks also appear in the beam in displacement cycles of 5 mm, 15 mm and 25 mm for specimen M2. For specimen P2, additional flexural cracks appear in the beam in displacement cycles of 7.5 mm, 10 mm and 15 mm. The first shear crack in the beam appears in the 7.5 mm displacement cycle for the specimen M2, and in the 5 mm displacement cycle for the specimen P2.

Table 1: Strength deterioration with increased displacement in the four specimens studied

Displacement, mm	*Average cycle strength in first cycle, kN*				*Strength deterioration, percent*							
					M1		*P1*		*M2*		*P2*	
					Repeat cycle		*Repeat cycle*		*Repeat cycle*		*Repeat cycle*	
	M1	*M2*	*M3*	*M4*	*1*	*2*	*1*	*2*	*1*	*2*	*1*	*2*
1.0	29.0	39.2	29.4	31.9	3.2	4.8	-0.5	-0.3	-10.6	2.1	2.5	-17.3
-1.0	-26.4	-36.9	-32.4	-32.3	0.9	0.3	0.8	-1.0	0.6	-1.4	9.2	6.9
2.0	48.0	66.9	48.4	61.1	3.1	4.4	-1.8	5.0	2.8	0.6	0.6	0.4
-2.0	-51.2	-60.9	-56.4	-53.5	1.6	1.7	-1.3	7.1	8.3	9.0	2.9	4.1
3.0	63.9	86.8	63.0	82.4	1.6	2.4	0.3	4.7	3.9	-0.7	-2.1	2.7
-3.0	-73.3	-76.7	-69.1	-67.6	1.3	1.8	3.8	2.5	4.1	4.1	1.9	4.5
5.0	88.2	118.9	88.6	117.2	2.0	2.3	2.5	4.2	-0.5	0.6	1.7	3.5
-5.0	-101.4	-102.5	-91.6	-96.7	1.7	1.1	0.5	6.1	4.7	5.6	5.4	6.5
7.5	114.9	153.5	118.4	154.7	1.8	2.2	3.5	5.7	1.9	3.5	2.7	2.9
-7.5	-126.3	-130.3	-118.3	-122.9	1.7	3.3	3.8	5.8	2.4	3.2	0.9	3.8
10.0	135.2	177.6	140.1	182.7	2.3	3.8	3.8	5.4	3.9	4.8	2.4	3.2
-10.0	-145.1	-150.3	-141.5	-145.7	2.4	3.5	3.5	6.3	3.2	4.6	3.0	4.7
15.0	164.6	218.9	169.2	228.1	4.3	5.7	5.6	10.5	2.0	3.7	2.8	4.0
-15.0	-169.9	-179.4	-168.9	-177.2	4.0	5.1	3.6	6.1	3.2	4.6	2.6	3.9
20.0	179.2	207.2	181.7	239.2	3.5	7.4	19.1	32.5	2.0	4.4	0.1	-0.1
-20.0	-182.2	-191.1	-181.2	-192.3	4.2	6.3	5.1	8.4	2.4	4.4	1.9	2.9
25.0	186.4	207.6	186.6	-	12.7	16.1	0.4	2.4	1.8	3.0	-	-
-25.0	-187.4	-203.4	-187.0	-199.8	3.2	7.0	2.8	6.2	2.2	3.2	1.9	3.1
30.0	173.5	251.3	189.2	-	5.7	30.9	4.7	6.4	1.8	3.5	-	-
-30.0	-187.7	-206.7	-186.2	-204.2	4.7	8.1	3.7	6.9	4.0	7.6	1.8	3.0
40.0	177.2	229.2	194.2	-	7.8	13.1	9.6	20.5	9.7	16.0	-	-
-40.0	-188.2	-212.3	-165.0	-212.2	7.8	12.7	5.8	9.0	8.7	14.7	2.6	3.3
50.0	172.0	-	-	-	9.0	16.2	-	-	-	-	-	-
-50.0	-181.6	-	-	-212.9	7.5	12.8	-	-	-	-	2.9	5.4
60.0	155.5	-	-	-	9.3	18.4	-	-	-	-	-	-
-60.0	-172.4	-	-	-208.8	9.4	14.4	-	-	-	-	3.4	6.0
70.0	135.2	-	-	-	7.2	14.0	-	-	-	-	-	-
-70.0	-160.4	-	-	-203.7	9.5	15.8	-	-	-	-	3.7	6.7

Results and discussions

Results

Hysteresis loops

The load-displacement hysteresis loops for the three cycles of loading at each displacement excursion level are shown in *Fig* 7. Maximum pinching was observed for the specimen M1, *Fig* 7*(a)* with predominant bond and shear failure in the joint region. Bond failure of U-shaped beam reinforcement and concrete in the joint occurred at the maximum displacement excursion level in the displacement cycles of 40 mm. This was accompanied by a steady degradation in strength.

Both the precast specimens, P1 and P2, showed increased stiffness in the direction of positive displacement due to the presence of corbels, *Fig*s 7*(b)* and 7*(d)*. Pinching was less compared to M1. Both the specimens show extensive flexural and shear cracking in beam with spalling of beam concrete at the column face for specimen P2. Only for the specimen P2, sliding of RC beam was observed along the through flexural crack at the face of the corbel. Longitudinal bar in the beam snapped, causing failure in the first cycle of 50 mm displacement for P1 and in the first cycle of 90 mm displacement for P2.

Specimen M2 exhibited fat hysteresis loops with very less pinching, due to good bonding between reinforcement and joint concrete. Shear cracks were also very few in the joint region. The cause of failure was the snapping of longitudinal beam bar in the first cycle of 50 mm displacement.

Strength

The strengths of the specimens in the first cycle of each displacement excursion level were observed, *Table* 1, and the strength deterioration in repeat cycles, with respect to the first cycle strength, were determined.

For specimen M1, the ultimate strengths in the positive and negative directions were about 186 kN and 188 kN, respectively. The test was stopped after completion of 70 mm displacement cycles, as the strength dropped below 80 percent of ultimate strength in positive displacement direction. The highest value of average strength deterioration is observed for the specimen P1.

For specimen M2, the ultimate strengths in the positive and negative loading directions were 194 kN and 197 kN respectively. The strength deterioration remained approximately at a steady value till a displacement level of 25 mm. For specimen P2, the ultimate strengths in the positive and negative loading directions were 239 kN and 213 kN, respectively.

Table 2: Stiffness degradation with increased displacement in the four specimens studied

Displacement, mm	Average cycle stiffness in first cycle, kN/mm.				Stiffness degradation, percent							
					M1		P1		M2		P2	
					Repeat cycle		Repeat cycle		Repeat cycle		Repeat cycle	
	M1	M2	M3	M4	1	2	1	2	1	2	1	2
±1	44.3	92.1	67.2	87.3	1.2	2.9	-0.1	1.7	1.6	3.5	13.1	3.8
±2	37.7	69.2	50.6	68.3	2.2	3.8	8.0	11.1	6.2	8.5	4.4	7.3
±3	33.7	51.5	38.7	51.6	3.3	4.0	7.5	10.8	5.1	7.7	4.8	8.0
±5	26.7	36.8	28.4	37.2	2.1	4.7	5.7	8.4	2.3	3.8	3.8	5.5
±7.5	22.0	29.0	23.6	30.0	4.5	5.4	5.7	8.6	3.8	5.6	3.7	5.3
±10	18.5	23.7	19.5	25.3	3.8	5.3	6.0	8.3	1.7	3.2	3.7	5.2
±15	13.8	18.0	15.1	19.4	5.1	6.8	5.7	10.5	4.1	6.5	4.0	6.1
±20	10.8	12.6	11.4	12.2	4.4	7.7	13.3	22.8	3.4	5.7	2.8	4.5
±25	8.7	10.4	8.9	9.8	9.5	13.0	2.2	5.0	2.7	4.6	2.5	4.0
±30	6.8	9.6	7.3	8.0	6.0	23.4	4.6	2.9	3.5	6.8	1.9	3.3
±40	5.0	7.9	5.0	6.0	8.5	13.9	8.1	16.1	10.3	17.3	2.8	4.0
±50	3.8	-	-	4.7	8.8	15.4	-	-	-	-	3.4	6.1
±60	2.9	-	-	3.8	9.9	16.9	-	-	-	-	3.7	6.6
±70	2.2	-	-	3.1	8.3	15.2	-	-	-	-	4.0	7.3

Stiffness

All the specimens showed sharp stiffness deterioration in the initial low displacement level, *Table* 2. The trend of stiffness degradation is similar to that of strength degradation except P2. For P2, the stiffness degradation attains a steady value after the displacement level of 42 mm. M1 and P1 showed less stiffness during the second repeat cycles than the first repeat cycle. Both M2 and P2 showed more stiffness than M1 and P1 respectively.

Energy dissipation

For all specimens, the energy dissipated in the first cycle of each displacement excursion level was greater than that in the subsequent cycles, with least energy dissipated in the last cycle. This is because most cracks at a particular displacement excursion level occurred in the first cycle; in the repeat cycles, these cracks marginally extended with very few new cracks appearing in the specimen. For P1, there was a sudden drop in energy dissipation in the 25 mm displacement cycle. This was due to the reduced damage incurred by the specimen between the two stages of testing, owing to increase in lever arm.

Specimens M1 and M2 showed regular increase of energy dissipated with the number of cycles. For M2, the decrease in energy dissipation in the repeat cycles was nearly uniform except for the third cycle of 40 mm displacement in which there is about 50 percent decrease in energy dissipation. For P2, there is not much difference in the energy dissipated in the repeat cycles, difference is maximum and of 10 percent in the last displacement excursion.

The variation of cumulative energy dissipated with the displacement level, *Fig* 8 showed a similar trend for all the specimens. Specimen M1 showed the maximum energy dissipation, thus indicating a ductile behaviour. This was further supported by the fact that the strain gauges attached to the longitudinal bars of beam and column for M2, recorded strains more than yield strain.

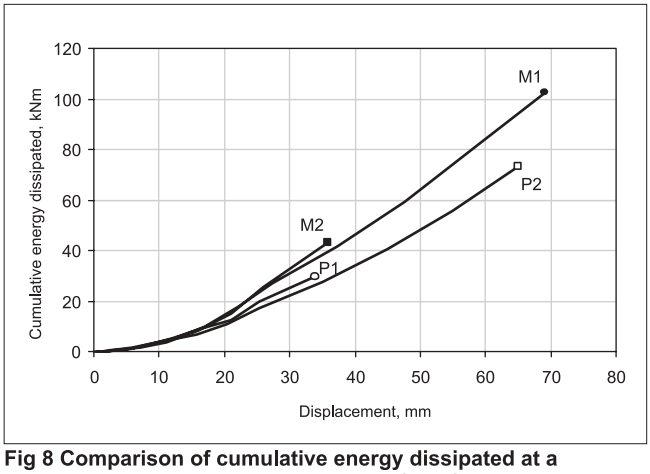

Fig 8 Comparison of cumulative energy dissipated at a displacement excursion level in each of the four specimens studied

Comparison of results and discussion

In all the four specimens, the displacement controlled loading was not applied at the same location in the beam. Hence, to compare the overall behaviour of the specimens, the hysteresis loops were derived for moment in the beam at the face of the column as function of transverse displacement applied at the end of the beam. The calculated flexural strength of the beam is 157.03 kN-m, while calculated overstrength is 15 percent. The specimens were compared for the different observed and calculated characteristics.

Comparison of specimen M1 and M2

(*i*) The pinching in hysteresis loops of the specimen M1 reflects predominant shear and bond failure, also corroborated by shear cracking in the joint, the gap between beam and column at the face of column, and the sub-yield strains in the longitudinal beam reinforcement. The relatively fat and stable loops of specimen M2 reflect predominant flexural failure, which is evident from the fewer shear cracks in the joint and snapping of beam reinforcement bar at failure.

(*ii*) The strength achieved in specimen M2, exceeds that obtained for the specimen M1. The strength and stiffness degradations in the second and third cycles for most displacement excursion levels, are higher for M1 compared to M2.

(*iii*) The cumulative energy dissipation for specimen M1 is more than that of specimen M2 after the 30 mm displacement cycles due to pinching in the hysteresis loops of M1.

Comparison of specimens M1 and P1

(*i*) Although the crack patterns extending into the columns in the joint region, are similar for both the specimens, the hysteresis loops of M1 show more pinching. The specimen P1 failed with the snapping of longitudinal reinforcement bar in the beam, while for specimen M1, failure is marked by the strength dropping below 80 percent in the post-ultimate response.

(*ii*) The ultimate strengths of both the specimens in the positive direction are nearly same, while in the negative direction, P1 has 11 percent more strength.

(*iii*) At low displacement levels, the specimen P1 has higher average strength and stiffness deterioration than the specimen M1.

(*iv*) The cumulative energy dissipated by the M1 is higher than that of P1 except at low displacement excursions. The energy dissipated by P1 may have been higher if the displacement in the positive direction was not restricted by the limitation in the force capacity of the actuator.

(*v*) Specimen M1 has a displacement ductility much higher than that of P1. The yield displacement of specimen M1 is nearly equal in both the directions, while in the specimen P1 the yield displacement in the positive direction is smaller than that of negative direction, because of higher stiffness due to corbel.

Comparison of specimen M2 and P2

(*i*) At higher displacement cycles, the specimen M2 has stable hysteresis loops than P2.

(*ii*) In the negative loading direction, P2 shows 12 percent higher strength than specimen M2. In the positive direction, P2 could not be loaded to its ultimate strength due to the restriction of applied displacement; thus it shows lower strength than M2 in that direction.

(*iii*) At low displacement level, M2 has less stiffness degradation than P2, while at higher displacement levels, the stiffness degradation increases for M2.

(*iv*) For both the specimens, maximum energy dissipated in the first cycle is the same. Till the 40 mm displacement cycle, which is the last displacement cycle sustained by M2, the cumulative energy dissipated by M2 is about 35 percent higher than specimen P2. However, at failure, the cumulative energy dissipated by specimen P2 is about 75 percent higher than specimen M2.

Comparison of specimen P1 and P2

(*i*) The hysteresis loops for specimen P2 show less pinching than those of specimen P1. Both specimens fail with the snapping of longitudinal beam bars. The damage in the specimen P2 is mostly concentrated in the beam with a few shear cracks in the joint, whereas in specimen P1, there is extensive shear cracking in the joint. In specimen P2, sliding of the beam takes place in higher displacement cycles, along the flexural crack at the face of the corbel, which does not occur in specimen P1.

(*ii*) The specimen P2 has marginally higher strength than the specimen P1 in both the directions. Strength and stiffness deterioration are greater in specimen P1 for both repeat cycles.

(*iii*) Till the maximum displacement cycle for P1, the cumulative energy dissipated by specimen P1 is about more than that of P2. But the maximum cumulative energy dissipated at failure by P2 is about 60 percent higher than that at its failure by P1. The displacement ductility factor achieved by the specimen P2 is about 32 percent higher than P1.

The above discussion shows that specimen P2 displays much better behaviour than specimen P1. But, from the construction point of view, specimen P1 is better as the joint detailing in it is much simpler than that in specimen P2. In the specimen P1, only the longitudinal reinforcement of columns are required to be welded, and no welding is required in the beam reinforcement as the top beam reinforcement bars continue as bottom bars through a U-turn within the joint. In contrast, the detailing of specimen P2 requires the longitudinal beam reinforcement to be continued into the column. To achieve this, L-shaped companion reinforcement bars are placed in both the column components, which are welded to the longitudinal bars in the beam component. Thus, welding is required in both the beam and the column reinforcement. The companion reinforcement bars in the column increase congestion in the joint and make the welding cumbersome.

Conclusions

The following are the salient conclusions drawn from the present study.

(*i*) The monolithic specimen with beam bars anchored into the column performed better than the monolithic specimen with continuous U-bars as beam reinforcement.

(*ii*) The precast specimen with beam bars anchored into the column performed better than the corresponding

Table 3: Displacement ductility of four specimens studied

Specimen	*Displacement excursion, mm*				*Displacement ductility*		*Average displacement ductility*
	Yield		*Ultimate*				
	+ *direction*	– *direction*	+ *direction*	– *direction*	+ *direction*	– *direction*	
M1	4.5	4.0	61.0	66.6	13.56	16.65	15.00
P1	2.5	3.5	21.0	33.0	8.40	15.71	12.00
M2	3.0	3.0	35.8	36.8	11.93	12.27	12.10
P2	2.0	4.0	15.0	65.0	7.50	16.25	11.88

monolithic specimen. This is attributed to the lapping of the beam and column bars in the former resulting in higher joint reinforcement. There was no weld failure.

(*iii*) The precast specimen with continuous U-bars as beam reinforcement performed worse than the corresponding monolithic specimen. This is attributed to the sliding of the beam stub at the interface with the beam-column joint, which was absent in the monolithic specimen.

(*iv*) Of the two precast specimens, the one with beam bars anchored into the column with welding of the lap splices performed better than the one with continuous U-bars as beam reinforcement.

Even though the joint detailing with the beam bars welded to the column bars is more involved, it is recommended for use in earthquake-resistant precast construction in high seismic regions.

Acknowledgement

This study is conducted as part of a research project under a technical collaboration programme in India between the Indian Institute of Technology Kanpur and the Central Building Research Institute (CBRI), Roorkee.

References

1. Englekirk,R.E. Seismic design considerations for precast concrete multistorey buildings, *PCI Journal*, 1990, pp. 40-51.
2. Fu, H.C and Seckin, M. Beam-column connections in precast concrete connections, *ACI Structural Journal*, 1990, pp. 252-261.
3. Cheok, G.S. and Lew, H.S. Performance of precast concrete beam-to-column connections subjected to cyclic loading, *PCI Journal*, 1991, pp. 56-67.
4. Amu, U., French, C.W. and Tarzikhan, C. Connection between precast elements- failure within connection region, *Journal of Structural Engineering*, ASCE, 1989, Vol. 115, No. 12, pp. 3171-3192.
5. _____*Code of practice for design and construction of floors and roofs using precast reinforced/prestressed concrete ribbed or cored slab unit*, IS 10297 : 1987, Bureau of Indian Standards, New Delhi
6. _____*Code of practice for construction for floors and roofs using precast concrete waffle units*, IS 10505 : 1983, Bureau of Indian Standards, New Delhi.
7. _____*Code of practice for construction with large panel prefabricates*, IS 11447 : 1985, Bureau of Indian Standards, New Delhi.
8. _____*Indian standard code for earthquake resistant design and construction of buildings,* IS 4326 : 1993, Bureau of Indian Standards, New Delhi.
9. _____FEMA 302-1997, (1997), *NEHRP Recommended Provisions for Seismic Regulation of New Buildings and other Structures*, Federal Emergency Management Agency, Report No. 302, Washington D.C., USA..
10. _____*Structural Engineering Design Provisions, Uniform Building Code 1997: Part 2,* International Conference of Building Officials, Whittier, CA, USA.
11. _____*Building code requirement for structural concrete,* ACI 318-1995, American Concrete Institute, MI, USA.
12. _____*Code of practice for the design of concrete structures and commentary*, NZS 3101, Part 1, (1995), Standards Association of New Zealand, Wellington.
13. _____*Code of practice for ductile detailing of reinforced concrete structures subjected to seismic forces, IS* 11447 : 1985, Bureau of Indian Standards, New Delhi.
14. Joshi, M.K. *Experimental Investigation of cyclic behaviour of precast RC exterior beam-column joints,* Master of Technology Thesis, Department of Civil Engineering, 2000, Indian Institute of Technology Kanpur, Kanpur.

Mr Manoj K. Joshi was formerly a master's student at the department of civil engineering at the Indian Institute of Technology (IIT) Kanpur.

Prof C.V.R. Murty is currently professor in the department of civil engineering at IIT Kanpur. His areas of interest include research on seismic design of steel and RC structures, development of seismic codes, modelling of nonlinear behaviour of structures and continuing education. He is a member of the Bureau of Indian Standards Sectional Committee on earthquake engineering and the Indian Roads Congress Committee on bridge foundations and substructures, and is closely associated with the comprehensive revision of the building and bridge codes.

Dr M.P. Jaisingh was formerly deputy director at the Central Building Research Institute, (CBRI) Roorkee. He was a member of the Bureau of Indian Standards Sectional Committee on housing and actively participated in the formulation of standards on precast construction.

●●●